NEOPLASIA
www.neoplasia.com

Volume 18 Number 12 December 2016 pp. 765–774 765

Suppression of Tumor Growth and Muscle Wasting in a Transgenic Mouse Model of Pancreatic Cancer by the Novel Histone Deacetylase Inhibitor AR-42[1,2]

Sally E. Henderson[*], Li-Yun Ding[†,‡], Xiaokui Mo[§], Tanios Bekaii-Saab[¶], Samuel K. Kulp[f], Ching-Shih Chen[#,] and Po-Hsien Huang[†,‡]**

*Department of Veterinary Biosciences, College of Veterinary Medicine, The Ohio State University, 1925 Coffey Rd., Columbus, OH, 43210, USA; [†]Department of Biochemistry and Molecular Biology, College of Medicine, National Cheng Kung University, 1 University Rd., Tainan 701, Taiwan; [‡]Institute of Basic Medical Sciences, College of Medicine, National Cheng Kung University, 1 University Rd., Tainan 701, Taiwan; [§]Center for Biostatistics, The Ohio State University, 1800 Cannon Drive, Columbus, OH, 43210, USA; [¶]Division of Medical Oncology, Department of Internal Medicine, Mayo Clinic, 5777 East Mayo Boulevard, Phoenix, AZ, 85054, USA; [#]Division of Medicinal Chemistry and Pharmacognosy, College of Pharmacy and Comprehensive Cancer Center, The Ohio State University, 500 West 12th Ave, Columbus, OH, 43210, USA; [**]Institute of Biological Chemistry, Academia Sinica, 128, Academia Road Sec. 2, Taipei City, 115, Taiwan

Abstract

PURPOSE: Pancreatic ductal adenocarcinoma (PDAC) is the third leading cause of cancer death in the United States. This study was aimed at evaluating the efficacy of AR-42 (formerly OSU-HDAC42), a novel histone deacetylase (HDAC) inhibitor currently in clinical trials, in suppressing tumor growth and/or cancer-induced muscle wasting in murine models of PDAC. *EXPERIMENTAL DESIGN:* The *in vitro* antiproliferative activity of AR-42 was evaluated in six human pancreatic cancer cell lines (AsPC-1, COLO-357, PANC-1, MiaPaCa-2, BxPC-3, SW1990). AsPC-1 subcutaneous xenograft and transgenic KP$^{fl/fl}$C (LSL-Kras^{G12D};Trp53$^{flox/flox}$;Pdx-1-Cre) mouse models of pancreatic cancer were used to evaluate the *in vivo* efficacy of AR-42 in suppressing tumor growth and/or muscle wasting. *RESULTS:* Growth suppression in AR-42–treated cells was observed in all six human pancreatic cancer cell lines with dose-dependent modulation of proliferation and apoptotic markers, which was associated with the hallmark features of HDAC inhibition, including p21 upregulation and histone H3 hyperacetylation. Oral administration of AR-42 at 50 mg/kg every other day resulted in suppression of tumor burden in the AsPC-1 xenograft and KP$^{fl/fl}$C models by 78% and 55%, respectively, at the end of treatment. Tumor suppression was associated with HDAC inhibition, increased apoptosis, and inhibition of proliferation. Additionally, AR-42 as a

Address all correspondence to: Ching-Shih Chen, Division of Medicinal Chemistry and Pharmacognosy, College of Pharmacy, The Ohio State University, USA. or Po-Hsien Huang, Department of Biochemistry and Molecular Biology, College of Medicine, National Cheng Kung University, Tainan 701, Taiwan.
E-mail: Henderson.451@osu.edu

[1] Conflict of Interest: C. S. C. is the inventor of AR-42, which was licensed to Arno Therapeutics, Inc., for clinical development by The Ohio State University Research Foundation. The other authors have no conflict of interest to declare.

[2] Financial support: Research reported in this publication was supported by: Lucius A. Wing Endowed Chair Fund from Ohio State University Comprehensive Cancer Center (C.S.C.)Bi-Institutional Collaborative Pancreatic Cancer Research grant from National Cheng Kung University College of Medicine (L.Y.D., P.H.H., C.S.C.) and The Ohio State University Wexner Medical Center and Comprehensive Cancer Center (T.B.S.), and grant # MOST 105-2321-B-001-064 from the Team of Excellent Research Program of the Ministry of Science and Technology, Taiwan (C.S.C.).National Institutes of Health grant T32OD010429-14 (S.E.H.)National Institutes of Health grant P30 CA016058, which supports, in part, the Target Validation Shared Resource at The Ohio State University Comprehensive Cancer Center.
Received 14 September 2016; Revised 20 October 2016; Accepted 20 October 2016

1476-5586
http://dx.doi.org/10.1016/j.neo.2016.10.003

single agent preserved muscle size and increased grip strength in $KP^{fl/fl}C$ mice. Finally, the combination of AR-42 and gemcitabine in transgenic mice demonstrated a significant increase in survival than either agent alone. *CONCLUSIONS:* These results suggest that AR-42 represents a therapeutically promising strategy for the treatment of pancreatic cancer.

Neoplasia (2016) 18, 765–774

Introduction

Pancreatic cancer is the third leading cause of cancer death in the United States [1]. Despite advances in chemotherapeutic regimens, prognosis remains dismal, with a 5-year survival of less than 7% for all stages [1] and a 5-year survival rate of only 2% among patients with metastatic disease [2]. Surgical resection followed by adjuvant therapy offers the only chance for a cure; however, less than 15% of patients present with resectable disease [3]. Cytotoxic chemotherapy with gemcitabine has been the standard of care and the backbone of experimental regimens in advanced pancreatic cancer for over a decade [4]. More recent studies have identified the benefit of nab-paclitaxel in combination with gemcitabine in marginally improving the median overall survival to 8.5 months versus 6 months with gemcitabine alone, and similar results were found in metastatic pancreatic cancer using a 5-flurouracil, oxaliplatin, and irinotecan regimen [2,5]. However, the overall poor median survival for this disease persists because of inherent or acquired drug resistance to cytotoxic agents. Therefore, there is an unmet need to develop novel therapies to improve clinical outcomes in pancreatic cancer.

The organization of the genome is defined by chromatin structure and regulates whether genes are actively transcribed or silenced. The epigenetic mechanisms that regulate chromatin structure and thus influence gene expression include methylation of cytosine bases in DNA and posttranslational modifications of histone proteins [6]. These histone modifications include acetylation, which is associated with open, actively transcribed chromatin, and deacetylation, which is associated with closed, or inactive, heterochromatin. The acetylation and deacetylation of histones are mediated by histone acetyltransferases and histone deacetylases (HDACs), respectively [6]. HDACs are often overexpressed in various types of cancer, resulting in increased proliferation and dedifferentiation [6,7], and their pharmacologic inhibition has been shown to have potent anticancer effects, including growth arrest, differentiation and apoptosis, in multiple types of human cancer cells [7,8], including pancreatic cancer. For example, trichostatin A [9] and suberoylanilide hydroxamic acid (SAHA, vorinostat, Zolinza) have been shown to inhibit the growth of various pancreatic cell lines alone and in combination with gemcitabine [10,11], and *in vitro* synergism was reported for the combination of chidamide, a novel benzamide HDAC inhibitor, and gemcitabine in inducing cell growth arrest and apoptosis in pancreatic cancer cell lines [12].

AR-42 is a novel HDAC inhibitor that was developed in our laboratory and is currently in Phase I/IB trials in both hematological malignancies and solid tumors [13]. The *in vivo* antitumor efficacy of oral AR-42 has been demonstrated by its ability to suppress the growth of various types of xenograft tumors in nude mice, including those of prostate [14], liver [15], ovary [16], and mast cells [17], as well as to block prostate carcinogenesis in a transgenic mouse model [18]. Evidence suggests that AR-42 mediates antitumor effects through both histone-dependent and -independent mechanisms. Aside from epigenetic activation of tumor suppressor genes, AR-42 has been shown to facilitate Akt dephosphorylation *via* phosphatase 1 (PP1) activation [19], to inhibit the gp130/Stat3 pathway [20], to inactivate the DNA repair machinery for double-strand breaks *via* Ku70 acetylation [21], to downregulate constitutively active Kit [17], and to facilitate the proteasomal degradation of topoisomerase IIα [22]. The safety profile of AR-42 has previously been established in the mouse prostate (TRAMP) model, where mild hematologic alterations and testicular degeneration were seen and found to be completely reversible following discontinuation of drug [18].

In addition to the aforementioned tumor-suppressive effects, the ability of AR-42 to reverse cancer-induced muscle wasting in the colon-26 carcinoma and Lewis lung carcinoma models of cachexia is noteworthy [23]. Cachexia, characterized by severe weight loss due to depletion of skeletal muscle mass that is not reversible by conventional nutritional support [24], is prevalent among pancreatic cancer patients [25] and contributes significantly to the morbidity and mortality of this disease. Based on these data, we hypothesized that AR-42 might also ameliorate the development of cachexia in PDAC in addition to suppressing tumor growth.

In the present study, we examined the *in vitro* effects of AR-42 in six human pancreatic cancer cell lines. We show that AR-42 demonstrates potent antiproliferative effects associated with dose-dependent modulation of apoptosis, HDAC inhibition, and decreased proliferation and G2 cell cycle arrest. The *in vivo* efficacy of AR-42 was demonstrated by suppression of tumor growth in an AsPC-1 tumor xenograft mouse model and a $KP^{fl/fl}C$ transgenic mouse model of pancreatic cancer. Tumor suppression in the xenograft tumors was associated with HDAC inhibition, increased apoptosis, and inhibition of proliferation. In addition, AR-42 as a single agent maintained muscle fiber size and increased grip strength in transgenic mice. Furthermore, the combination of AR-42 and gemcitabine showed a significant improvement in survival over the use of either agent alone. These results suggest that the use of AR-42 represents a therapeutically promising strategy for the suppression of tumor growth in pancreatic cancer.

Materials and Methods

Reagents

AR-42 was a kind gift from Arno Therapeutics, Inc. (Flemington, NJ). For *in vitro* experiments, a stock solution of AR-42 was prepared in dimethyl sulfoxide (DMSO) and diluted in a 10% serum-containing culture medium for treatment of cells (final concentration of DMSO <0.1%). For *in vivo* experiments, AR-42 was prepared as a suspension in a vehicle [10% DMSO, 0.5%

methylcellulose (wt/vol) and 0.1% Tween 80 (vol/vol) in sterile water] for oral administration to xenograft-bearing athymic nude mice. Antibodies and primer sequences are listed in the Supplementary Information.

Cell Culture

Human pancreatic cancer cell lines PANC-1, AsPC-1, BxPC-3, SW1990, and MiaPaCa-2 were purchased from American Type Culture Collection (Manassas, VA), which authenticates human cell lines in their collection using short tandem repeat analysis, and were used in fewer than 6 months of continuous passage. The COLO-357 human pancreatic cell line was obtained from the Tissue Culture Shared Resource of Georgetown Lombardi Comprehensive Cancer Center (Washington, D.C.) where DNA fingerprinting was performed for authentication. PANC-1, SW1990, BxPC-3, AsPC-1, and COLO-357 cells were cultured in RPMI 1640 medium (Gibco, Life Technologies, Grand Island, NY) supplemented with 10% fetal bovine serum (FBS; Gibco, Life Technologies) and 1% penicillin-streptomycin. MiaPaCa-2 cells were cultured in Dulbecco's modified Eagle's medium (DMEM; Gibco, Life Technologies) supplemented with 10% FBS and 1% penicillin-streptomycin. All cells were cultured at 37°C in a humidified incubator containing 5% CO_2. Cells in log phase growth were harvested by trypsinization for use in various assays and *in vivo* studies.

Analyses of Cell Viability and Cell Cycle

Cell viability was assessed with 3-(4,5-dimethylthiazol-2-yl)-2,5-diphenyltetrazolium bromide (MTT) assays as described previously [14]. Cell cycle analysis was performed by using standard methods as described previously [26]. Further experimental details are included in the Supplementary Information.

Immunoblotting

Western blot analyses of AR-42– and vehicle-treated pancreatic cancer cells were performed as previously reported [19]. Briefly, 3×10^5 cells were seeded onto 6-cm plates in 10% FBS–supplemented medium. After 24 hours, cells were treated with AR-42 for 48 hours in the same medium and then suspended in SDS lysis buffer, sonicated, and boiled for 10 minutes. Equivalent amounts of protein lysates were resolved by SDS-PAGE (10%-12%); transferred to nitrocellulose membrane; and immunoblotted for phospho-Akt (Ser473), Akt, PCNA, cleaved PARP, BAK, BCL-X_L, c-Myc, cyclin B1, p21, acetylated histone H3, and histone H3. Western blot analysis of equivalent amounts of muscle protein lysates from $KP^{fl/fl}C$ mice were resolved by SDS-PAGE as described above and immunoblotted for Murf-1, acetylated histone H3, and histone H3.

AsPC-1 Xenograft Tumor Model

Female athymic nude mice (5 weeks of age) were obtained from the Target Validation Shared Resource of The Ohio State University Comprehensive Cancer Center. Each mouse received a subcutaneous injection of 1×10^6 AsPC-1 cells in a total volume of 0.1 ml of serum-free medium containing 50% Matrigel (BD Biosciences, San Jose, CA) under isoflurane anesthesia. As the tumors became established (90.7 ± 9.4 mm^3 [mean, SD]), the mice were randomly divided into two groups ($n = 7$) that received the following treatments by oral gavage every other day: vehicle (0.5% methylcellulose/0.1% Tween 80/10% DMSO in water) and AR-42 at 50 mg/kg of body weight. Tumors were measured weekly with calipers, and their volumes were calculated with a standard formula: width^2 × length × 0.52. Body weights were measured weekly. At termination, tumors were harvested, snap-frozen in liquid nitrogen, and stored at −80°C until biomarker analysis by Western blotting. Procedures were performed in accordance with protocols approved by the Institutional Animal Care and Use Committee of The Ohio State University.

Genetically Engineered Mouse Model of Pancreatic Cancer

To assess the effects of AR-42 on tumor growth, cancer-induced muscle wasting, and gemcitabine sensitivity in a spontaneous tumor model of pancreatic cancer, each of the $KP^{fl/fl}C$ (LSL-$Kras^{G12D}$;$Trp53^{flox/flox}$;Pdx-1-Cre) mice was verified by genotyping PCR and screened for the presence of pancreatic tumors by ultrasound at 4 weeks of age, and randomized to groups (n = 7-16) that received the following treatments: (a and b) AR-42 alone (25 and 50 mg/kg, q2d, p.o. by gavage); (c and d) gemcitabine alone (40 and 80 mg/kg, twice weekly, i.p.); (e) AR-42 (25 mg/kg, q2d, p.o.) plus gemcitabine (40 mg/kg, twice weekly, i.p.); and (f) vehicles (0.5% methylcellulose/0.1% Tween 80/10% DMSO in water, p.o., and physiological saline, i.p.). AR-42 and gemcitabine were administered continuously for the entire study. Tumor volumes were calculated from biweekly ultrasound measurements with a Vevo 770 instrument and a 60-MHz probe (Visualsonics Inc. Ontario, Canada) in anesthetized mice. At terminal sacrifice, tumors were harvested and bisected with one piece preserved in RNAlater reagent (Qiagen, Valencia, CA) for RNA and biomarker analyses and the other piece fixed in formalin and embedded in paraffin for histological and immunohistochemical analysis. Hindlimb muscles (gastrocnemius, quadriceps, tibialis anterior) were also harvested for evaluation of muscle fiber size, as described below in "Grip Strength Analysis and Cross-Sectional Area of Muscle Fibers." All experimental procedures using live animals were conducted in accordance with protocols approved by The National Cheng Kung University Institutional Animal Care and Use Committee.

Immunohistochemical Analysis

All tissues were examined *via* light microscopy using an Olympus Model BX53 microscope (Olympus Corp., Tokyo, Japan). The hematoxylin and eosin (H&E) staining of pancreatic tumor sections from each $KP^{fl/fl}C$ mouse was performed according to standard procedures. To evaluate pancreatic epithelial proliferation, 5-mm-thick, paraffin-embedded tissue sections of the tumorous pancreas were immunostained for pan-cytokeratin AE1/AE3 (GTX26401, GeneTex, Hsinchu City, Taiwan) applied at the dilution of 1:500. The immunohistochemistry (IHC) staining protocol used the EnVision Detection Systems Peroxidase/DAB staining technique per manufacturer's instructions (K5007; Dako, Glostrup, Denmark). Staining is completed by a 5- to 10-minute incubation with 3-amino-9-ethylcarbazole chromogen, which results in a pink-colored precipitate at the antigen site.

Opal Multiplexed IHC

Pancreatic tumors from KPC mice were formalin fixed and paraffin embedded for Opal multiplexed IHC staining. Pancreatic tissue sections of 5 μm thickness were deparaffinized, rehydrated and the antigen retrieval were performed in microwave to boil for 25 minutes using Opal antigen retrieval buffer at pH = 6.0 (Opal 4-color IHC Kit, NEL79400, Perkin Elmer, Inc., Waltham, MA). All tissue sections were blocked with antibody diluent (Dako, S0809,

Carpinteria, CA) for 10 minutes at room temperature. Sections were then incubated with primary antibodies (Ki67 and pan-cytokeratin [GeneTex Inc., Hsinchu City, Taiwan] and caspase-3 [Santa Cruz Biotechnology, Inc. Dallas, TX]) overnight at 4°C followed by incubation with HRP-conjugated secondary antibodies (Dako, K5007, Carpinteria, CA) for 10 minutes at room temperature. A 50× diluted TSA Plus Working Solution (Opal 4-color IHC Kit, NEL79400) was added to slides to incubate for 10 minutes at room temperature. Slides were stripped using microwave, blocked, and then incubated with primary antibodies, HRP-conjugated secondary antibodies, and TSA Plus Working Solution to amplify signals as described above. All primary antibodies were diluted with antibody diluent. DAPI was used to stain cell nuclei. Positive signals were quantified using ImageJ software with the same threshold. Three 20× individual fields for each sample were analyzed, and results were expressed as percentage per visual field.

Grip Strength Analysis and Cross-Sectional Area of Muscle Fibers

Forelimb grip strength was measured as previously described [23] using a Digital Grip Strength Meter (Columbus Instruments, Columbus, OH). For each mouse, grip strength was defined as the average of nine measurements. For evaluation of muscle fiber size, fresh frozen muscle tissues were prepared according to standard procedures. Essentially, the gastrocnemius, quadriceps, and tibialis anterior muscles were harvested by dissection under a Leica Wild M650 surgical microscope (Leica Microsystems [SEA] Pte Ltd., Singapore, Singapore) within 10 minutes after mice were sacrificed. The freshly isolated muscle tissues were rinsed with FSC 22 tissue freezing medium (Leica Microsystems [SEA], Pte Ltd., Singapore, Singapore) and placed into isopentane that was precooled in liquid nitrogen. The resulting frozen muscle cores were stored at −80°C. Cryosections of muscle cores were cut on a cryostat microtome (CM3050S, Leica Microsystems), paraffin embedded, and then H&E stained. Image J software [27] was used to calculate the cross-sectional areas of muscle fibers in three independent 400× fields in each muscle tissue section. Data were collected from 150 fibers from multiple sections of 6 mice per group.

Statistical Analysis

All analyses were performed at the OSU Center for Biostatistics by using SAS 9.4 (SAS, Inc., Cary, NC). Multiplicity was adjusted by using Holm's method to control the type I familywise error rate at 0.05. Analysis of variance (ANOVA) was used to analyze the cell line data, and dose dependencies were tested by trend analysis. Grip strength, and tumor growth for both xenograft and genetically engineered mouse models were analyzed by using mixed effect model, accounting for the association of the same measure at different time points from the same mouse. These models included treatment and time of the treatment as fixed factors, and the intercept of an individual mouse was considered as a random effect. Tumor weights were compared by using ANOVA, and percent of Ki67 immunopositivity and percent tumor areas were analyzed by 2-sample *t* tests. The survival functions were estimated by using Kaplan-Meier method, and the significant difference between survival probabilities among treatment groups was compared by log-rank tests. To test the association between treatment and the distribution of muscle fiber size, muscle fibers were dichotomized into two categories according to the ranges of the cross-sectional area (0-1800 μm^2, >1800 μm^2). We averaged the numbers of fibers of each range for each group and then used χ^2 to test the association.

Results

Potent Antiproliferative Effects of AR-42 in Human Pancreatic Cancer Cell Lines by Targeting Signaling Effectors Associated with the Regulation of Cell Survival and Cell Cycle Progression

Six human pancreatic cancer cell lines (AsPC-1, SW1990, BxPC-3, COLO-357, MiaPaCa-2, and PANC-1) were exposed to different concentrations of AR-42 for 72 hours, and cell viability was assessed with MTT assays. Among these cell lines, AsPC-1, SW1990, BxPC-3, COLO-357, and MiaPaCa-2 showed dose-dependent suppression of growth at sub-μM concentrations of AR-42, with IC_{50} values ranging from 0.4 to 0.5 μM (Figure 1, *A–E*). Pharmokinetic analysis of AR-42 *in vivo* demonstrates a C_{max} of 14.7 μM, well above the antiproliferative doses seen *in vitro* [28]. In contrast, PANC-1 cells were more resistant to AR-42 (IC_{50}, 6 μM) (Figure 1*F*). Nonetheless, AR-42 induced significant dose-dependent decreases in cell viability in all cell lines tested (all P values < .0001, trend tests). Western blot analysis of biomarkers of HDAC inhibition revealed concentration-dependent increases in the abundance of acetylated histone H3 and the cyclin-dependent kinase inhibitor p21 in all six cell lines examined, confirming HDAC inhibitory effects of AR-42 (Figure 2). The AR-42–mediated inhibition of cell viability was, in part, attributable to apoptosis, as evidenced by PARP cleavage, which was accompanied by parallel changes in the expression/phosphorylation levels of various apoptosis regulators, including Akt, the proapoptotic regulator BAK, and the antiapoptotic regulator Bcl-xL (Figure 2). Changes in these biomarkers were noted in the AR-42–resistant PANC-1 cells even at low concentrations of AR-42. In addition, AR-42 reduced the expression of several cell cycle regulators, including c-Myc and cyclin B1 in all six cell lines and PCNA, a protein involved in DNA replication, in AsPC-1, BxPC-3, and MiaPaCa-2 cells. Cell cycle analysis revealed that AR-42 induced G2/M arrest in AsPC-1, SW1990, BxPC-3, COLO-357, and PANC-1 cells consistent with the downregulation of cyclin B1 expression observed by Western blot. In MiaPaCa-2 cells, a prominent increase in treated cells in sub-G1 phase relative to control cells was observed, indicative of apoptosis (Supplementary Figure S1).

AR-42 Suppressed AsPC-1 Xenograft Tumor Growth In Vivo

The *in vivo* efficacy of AR-42 was assessed in a subcutaneous xenograft tumor model of pancreatic cancer. Female athymic nude mice bearing established AsPC-1 tumors (mean ± SD, 90.7 ± 9.4 mm^3) were treated with 50 mg/kg AR-42 or vehicle (n = 7 in each group) by oral gavage every other day. As shown in Figure 3*A*, AR-42 significantly suppressed AsPC-1 tumor growth. The growth in tumor volume at each of the time points examined was significantly lower in the AR-42–treated group than in the vehicle-treated group [7 days, (P < .05), 14 days (P < .0001), and 21 days (P < .0001) of treatment], culminating in a 78% reduction in tumor growth at the study end point. To correlate the suppression of tumor growth with the observed *in vitro* results, the effects of AR-42–mediated HDAC inhibition on representative intratumoral biomarkers of drug activity were evaluated by Western blotting of tumor lysates collected at the end of the study. Consistent with the *in vitro* findings, tumor suppression was associated with increased acetylation of histone H3 and changes in the expression of the apoptosis regulators BCL-X_L and BAK and the cell cycle regulators c-Myc, PCNA, and cyclin B1 (Figure 3*B*).

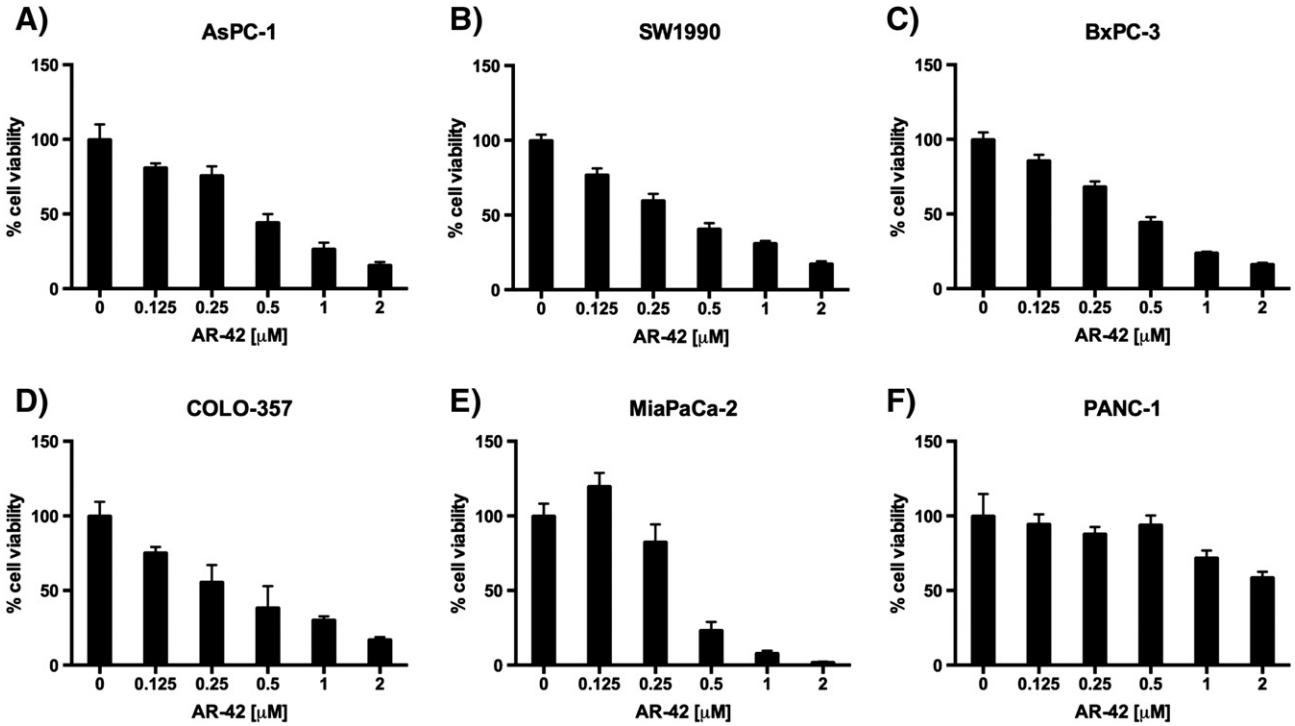

Figure 1. Antiproliferative effects of AR-42 in six different pancreatic cancer cell lines. Human PDAC cell lines (A) AsPC-1, (B) SW1990, (C) BxPC-3, (D) COLO-357, (E) MiaPaCa-2, and (F) PANC-1 were treated for 72 hours with AR-42 (Arno Therapeutics, Inc., Flemington, NJ). Cell viability was measured *via* MTT assay. The data are shown as mean ± SD of $n = 6$ replicates.

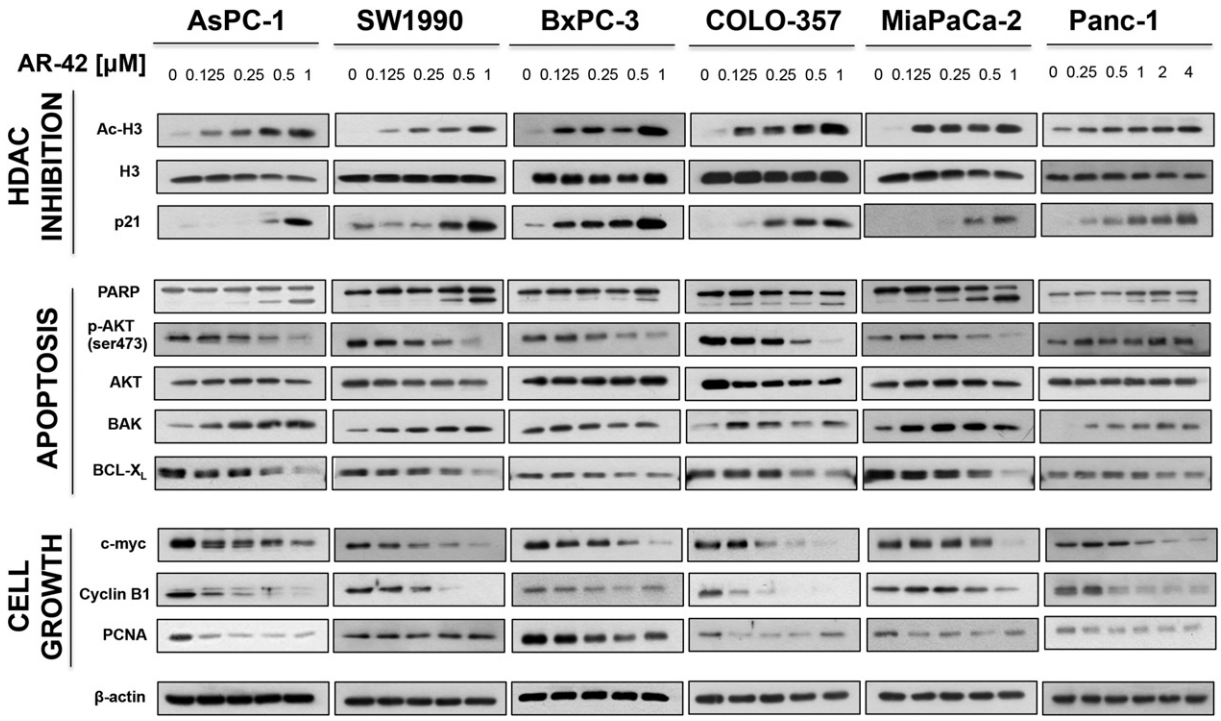

Figure 2. Effects of AR-42 on various biomarkers of apoptosis, HDAC inhibition, and proliferation. Human PDAC cells (AsPC-1, SW1990, BxPC-3, COLO-357, and PANC-1) were treated with AR-42 for 48 hours at the concentrations indicated, and cell lysates were made for Western blotting. Immunoblots of markers of HDAC inhibition (A), apoptosis (B), and proliferation and G2 cell cycle arrest (C). β-Actin was used as a loading control.

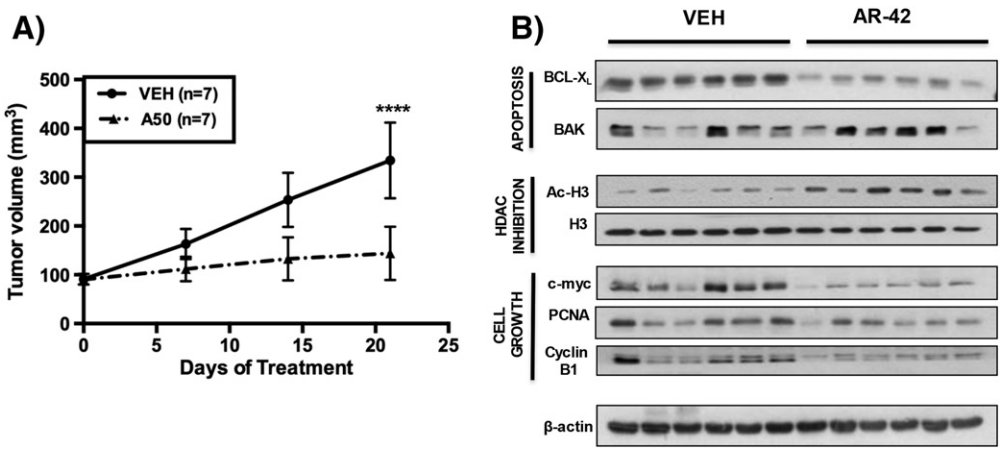

Figure 3. Effects of oral AR-42 in an AsPC-1 subcutaneous xenograft mouse model on tumor suppression and expression of intratumoral biomarkers of drug activity. Female athymic nude mice (5 weeks of age) were injected subcutaneously with 1×10^6 AsPC-1 cells. As the tumors became established (90.7 ± 9.4 mm3 [mean ± SD]), mice were treated with 50 mg/kg AR-42 ($n = 7$) or vehicle ($n = 7$) by oral gavage every other day. Tumor volume was measured weekly with calipers, and volumes were calculated with a standard formula: width^2 × length x 0.52. (A) AR-42 reduced tumoral volume by 78% after 21 days of treatment (****$P < .0001$). (B) Effects of HDAC inhibition on representative intratumoral biomarkers of drug activity evaluated through Western immunoblotting of AsPC-1 tumor homogenates collected after 21 days of treatment. β-Actin was used as a loading control. Tumor volumes were analyzed by mixed effect model, incorporating repeated measures for each tumor (from day 0 to 21).

AR-42 Suppressed Tumor Growth in a Genetically Engineered Model of Pancreatic Cancer

Pursuant to the above finding, we used the KP$^{fl/fl}$C (LSL-Kras^{G12D}; Trp53$^{flox/flox}$;Pdx-1-Cre) mouse model, which recapitulates the functional heterogeneity of human pancreatic cancer [29] to evaluate the *in vivo* efficacy of AR-42. Twenty-eight-day-old mice were treated with vehicle ($n = 11$) or AR-42 at 25 ($n = 7$) or 50 mg/kg ($n = 11$) by oral gavage every other day until sacrifice (Figure 4*A*). Ultrasound measurements of tumor volume demonstrated that AR-42 at 50 mg/kg significantly decreased tumor growth by 55% after 4 weeks of treatment (8 weeks of age) ($P < .05$) (Figure 4*B*), which was paralleled by reductions of 57.4% and 55.8% in the total weights of tumoral pancreas at the study end point in mice treated with AR-42 at 25 and 50 mg/kg, respectively ($P < .0001$ for both dosages) (Figure 4*C*). Immunohistochemical analysis of pancreatic tumors showed that treatment with AR-42 significantly decreased the percent of tumor area (pan-cytokeratin staining) ($P < .05$) (Figure 4*D*). Analysis of pancreatic tumors using immunofluorescence showed that treatment with AR-42 significantly decreased the percentage of proliferative tumor cells ($P < .001$) (Figure 4*F*) and increased percent caspase 3 area ($P < .05$) (Figure 4*G*).

The Combination of AR-42 with Gemcitabine Prolonged Overall Survival in KP$^{fl/fl}$C Mice Compared to Either Agent Alone

In light of the *in vivo* efficacy of AR-42 as a single agent, we assessed the ability of AR-42 to enhance the therapeutic effect of gemcitabine, a standard-of-care chemotherapeutic agent for pancreatic cancer, on the survival of KP$^{fl/fl}$C mice (Figure 5*A*). As shown, gemcitabine at 40 ($n = 8$) or 80 mg/kg ($n = 7$) (twice weekly, i.p.) and AR-42 at 25 ($n = 8$) or 50 mg/kg ($n = 12$) (q2d, p.o.) significantly prolonged the overall survival of KP$^{fl/fl}$C mice relative to vehicle control ($n = 16$) ($P < .05$ for all groups) (Figure 5*B*). The median survival times for these groups were as follows: vehicle, 59 days; AR-42: 25 mg/kg, 65 days; 50 mg/kg, 65 days; gemcitabine: 40 mg/kg, 68 days; 80 mg/kg, 75 days. The difference in survival between the low- and high-dose groups of either AR-42 or gemcitabine was not statistically significant. Therefore, a low-dose metronomic regimen consisting of every-other-day administration of AR-42 at 25 mg/kg and twice-weekly administration of gemcitabine at 40 mg/kg was used to examine the effect of the combination therapy on survival of KP$^{fl/fl}$C mice ($n = 9$). As shown, this drug combination significantly prolonged survival (median survival time, 83 days) relative to that for each single agent regimen (AR-42, $P < .0001$; gemcitabine, $P < .05$).

AR-42 Preserved Muscle Fiber Size and Grip Strength in KP$^{fl/fl}$C Mice

We recently reported that AR-42 suppressed cancer-induced muscle wasting in the C-26 colon carcinoma and Lewis lung carcinoma models of cancer cachexia [23]. Pursuant to this finding, we examined two indicators of skeletal muscle wasting, muscle fiber size and grip strength, in KP$^{fl/fl}$C mice treated with either AR-42 (25 mg/kg, q2d) or vehicle as described in the timeline shown in Figure 5*A*. Consistent with our previous work, AR-42 preserved muscle fiber size relative to vehicle, as determined by morphometric analysis of H&E-stained gastrocnemius muscle (Figure 6, *A* and *B*). The muscles of AR-42–treated mice contained a significantly greater proportion of fibers with large cross-sectional area (>1800 μm^3) than those of vehicle-treated mice (47.0% vs. 23.1%, $P < .001$) (Figure 6*B*). This finding was consistent with the grossly evident preservation of muscle size in AR-42–treated mice (Figure 6*A* and Supplementary Figure S2). Treatment with AR-42 resulted in an improvement in grip strength from 4 to 8 weeks of age ($P < .05$), whereas vehicle-treated mice showed decrease in grip strength over the same interval ($P < .05$). This anticachectic effect was reflected in the ability of AR-42 to improve grip strength at 8 weeks of age (4 weeks of treatment) versus vehicle control ($P < .01$) (Figure 6*C*). Furthermore, treatment with AR-42 resulted in decreased expression of the cachexia biomarker MuRF1 due to HDAC inhibition

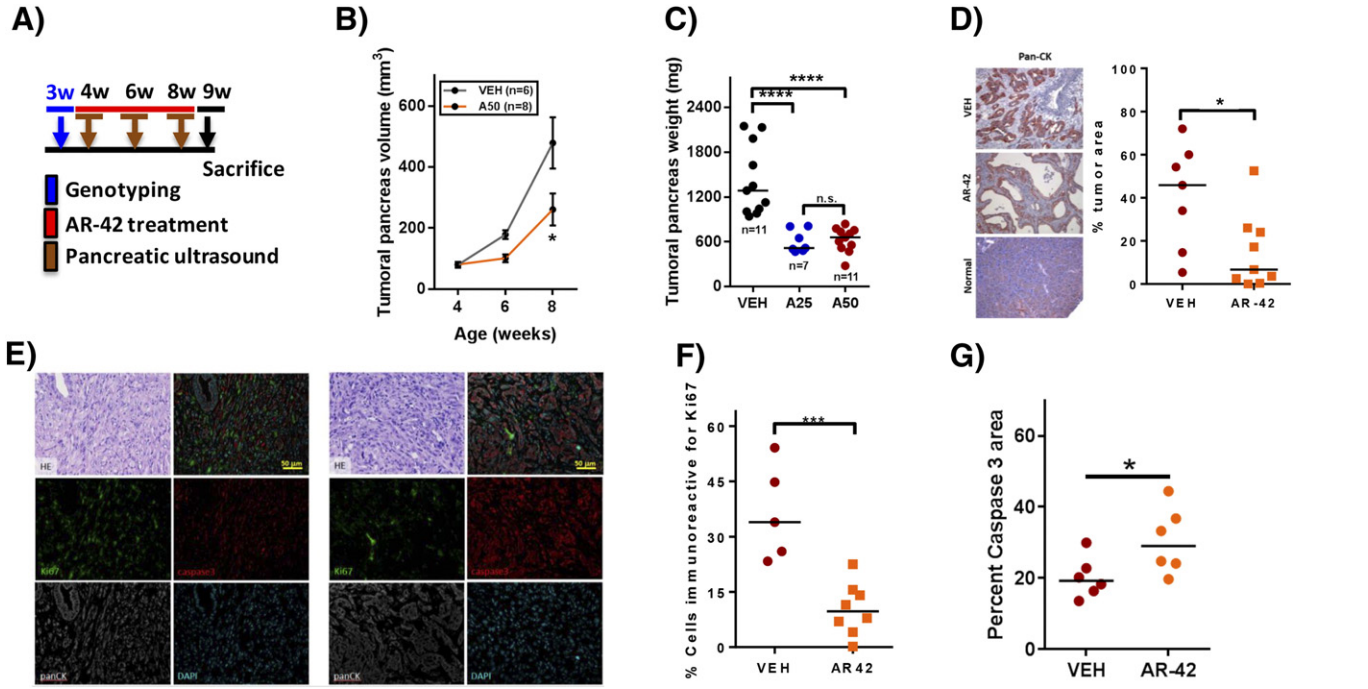

Figure 4. Effects of oral AR-42 in a transgenic mouse model of pancreatic cancer. (A) KP$^{fl/fl}$C (LSL-Kras^{G12D};Trp53$^{flox/flox}$;Pdx-1-Cre) genetically engineered mice at 4 weeks of age were treated with AR-42 at the 25- and 50-mg/kg dosage (n = 7 and 11, respectively) or vehicle (n = 11) by oral gavage every other day for 32 days. (B) Tumor volume was measured in mice using pancreatic ultrasound (Vevo 770) while mice were under anesthesia at weeks 4, 6, and 8. AR-42 (50 mg/kg) decreased the size of tumoral pancreas by 55% at week 8 (*P < .05). (C) *Ex vivo* pancreatic tumors were weighed postmortem at week 9. AR-42 decreased the total weight of the tumoral pancreas by 57.4% and 55.8% at the dosage of 25 and 50 mg/kg, respectively (****P < .0001). (D) Treatment with AR-42 significantly decreased the percent tumor area of the pancreas as evidenced by decreased pan-cytokeratin (AE1/AE3) immunostaining (*P < .05). (E) Immunofluorescence triple staining with pan-cytokeratin, Ki67, and active caspase 3. (F and G) The quantification of Ki67 and active caspase 3. Tumor weights were compared by using ANOVA; percent of Ki67+, percent tumor areas, and percent caspase 3 area were analyzed by two-sample t tests (*P < .05; ***P < .001). Note: n.s.: not significant.

demonstrated by increased expression of acetylated histone H3 (Figure 6*D*).

Discussion

Pancreatic cancer is associated with a dismal prognosis with few therapeutic options. HDAC overexpression has been documented in a variety of cancers, including pancreatic cancer [30], and therefore represents a promising target in pancreatic cancer therapy. Here, we demonstrate the *in vitro* and *in vivo* effects of the HDAC inhibitor AR-42 in pancreatic cancer. Our results show that AR-42 inhibits the growth of human pancreatic cancer cells at sub-μM concentrations in association with dose-dependent modulation of apoptotic regulators, HDAC inhibition, decreased proliferation, and G2 cell cycle arrest. Moreover, we show that AR-42 suppresses tumor growth in two mouse models of pancreatic cancer and ameliorates cancer-induced muscle atrophy.

A major mechanism in the pathogenesis of pancreatic cancer is evasion of apoptosis and acquisition of a drug-resistant phenotype [31]. In particular, the antiapoptotic factor BCL-X_L is overexpressed in pancreatic cancer, blocking activation of the intrinsic and extrinsic apoptosis pathways [32]. Treatment with AR-42 induced dose-dependent downregulation of BCL-X_L at sub-μM concentrations in all cell lines except PANC-1, where downregulation was noted at a concentration of 2 μM. In addition, AR-42 induced upregulation of the proapoptotic factor BAK and PARP cleavage at sub-μM doses in all cell lines. The PI3K/Akt pathway is an important prosurvival pathway in pancreatic cancer cells and is activated by oncogenic KRAS, as well as through growth factors and cytokines. Activation of PI3K leads to phosphorylation of Akt and subsequent antiapoptotic effects and uncontrolled cellular proliferation [31]. Furthermore, mutations in Akt in addition to KRAS mutations may accelerate PDAC development [33]. Recently, targeting the PI3K/Akt pathway in combination with blockade of MAPK has been shown to increase cell cycle arrest and apoptosis in pancreatic cancer cell lines [34]. We previously reported that AR-42 induces dephosphorylation of Akt through release of PP1 from PP1-HDAC complexes independent of histone acetylation [19]. In this study, AR-42 treatment resulted in dose-dependent downregulation of phospho-Akt in all cell lines except PANC-1. In addition to modulation of apoptosis, Akt regulates several transcription factors, including c-Myc [31], a proto-oncogene that when overexpressed leads to dysregulation of proliferation, differentiation, and apoptosis. It is estimated that c-Myc is overexpressed in 20% of all human cancers, including pancreatic cancer, and has been correlated with worse survival in pancreatic cancer patients [35]. We show that AR-42 induced potent downregulation of c-Myc in all cell lines tested. AR-42 treatment was also associated with decreased expression of cyclin B1, a regulatory protein involved in the transition from the G2 to M phase of the cell cycle. Overexpression of cyclin B1 leads to uncontrolled binding to cyclin-dependent kinases, resulting in

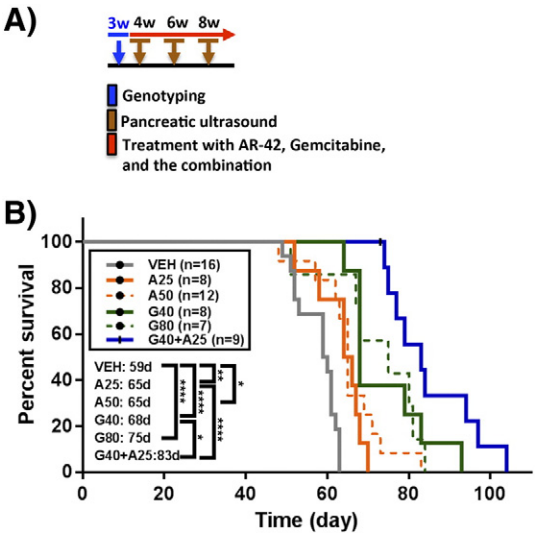

Figure 5. Kaplan-Meier survival curves. (A) Timeline of gemcitabine and AR-42 administration. (B) AR-42 alone (25 mg/kg [A25], p.o., every other day, $n = 8$ and 50 mg/kg [A50] p.o. every other day, $n = 12$), gemcitabine alone (40 mg/kg [G40] by i.p. injection twice weekly, $n = 8$ and 80 mg/kg [G80] by i.p. injection twice weekly; $n = 7$), and the combination of both gemcitabine and AR-42 (G40 + A25; $n = 9$) significantly increased survival in KPC mice compared to mice treated with vehicle ($n = 16$). The combination of AR-42 at 25 mg/kg and gemcitabine at 40 mg/kg significantly increased the median survival time (83 days) relative to AR-42 ($P < .0001$) and gemcitabine ($P < .05$) alone. Statistical comparison of survival curves was performed with log-rank test (*$P < .05$; **$P < .01$; ****$P < .0001$).

unregulated proliferation [36], and has been linked to mutations in the tumor suppressor p53, which occurs in 50% to 75% of pancreatic cancer patients [37,38]. Mutant p53 has also been implicated in driving rapid progression of premalignant lesions with $KRAS^{G12D}$ mutations, promoting malignant tumor growth and metastasis [38]. Therefore, AR-42 appears to target pathways downstream of oncogenic KRAS and those associated with mutations frequently seen in pancreatic cancer, demonstrating a spectrum of antitumor activity that is reflected in its broad efficacy against five different pancreatic cancer cell lines and that suggests its potential clinical activity against PDAC.

Our data showed that PANC-1 cells were more resistant to AR-42 than the other cell lines tested, which is consistent with previous reports of PANC-1's resistance to other HDAC inhibitors, including SAHA, trichostatin A, and panobinostat [9,11,39]. For instance, it was reported that SAHA did not inhibit proliferation, had no significant effect on PARP cleavage or caspase-3, and failed to induce expression of p21 in PANC-1 cells, leading the authors to conclude that the major mechanism by which SAHA induces growth arrest in some pancreatic cancer cell lines is dependent on p21 upregulation [11]. In our study, however, despite sensitivity to AR-42–induced upregulation of p21 at sub-μM concentrations and to HDAC inhibition as indicated by increased acetylated-H3, PANC-1 cells were markedly more resistant to the antiproliferative effects of AR-42 ($IC_{50} > 2$ μM). The lack of Akt dephosphorylation and the need for a higher dose of AR-42 to downregulate $BCL\text{-}X_L$ expression in PANC-1 cells may suggest a mechanism by which this cell line is more resistant to HDAC inhibitors. Characterizing the molecular

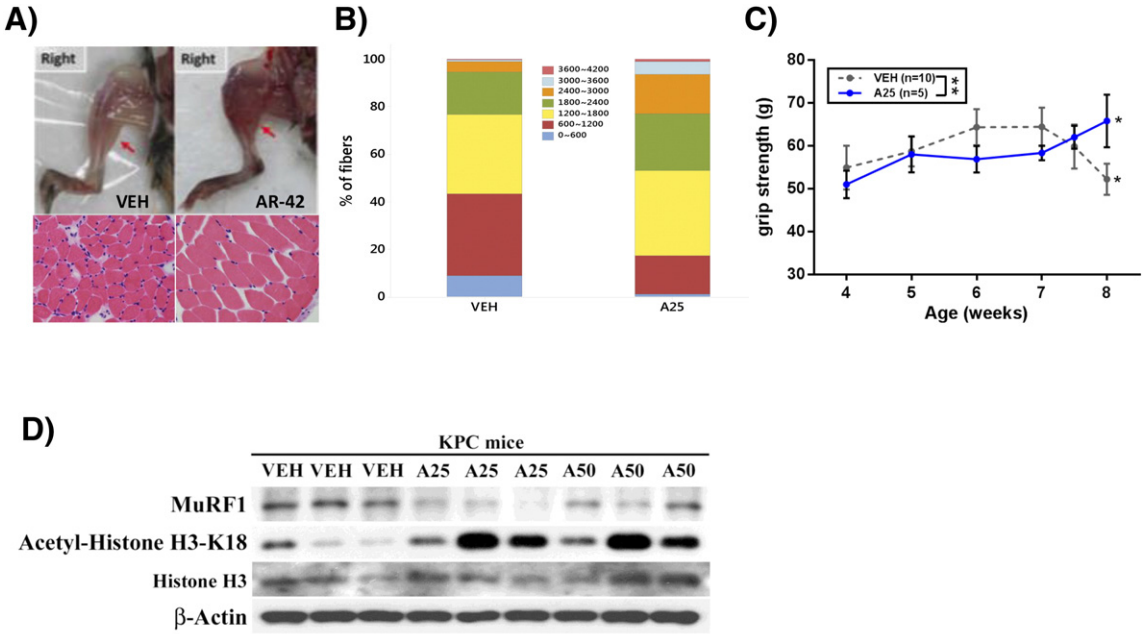

Figure 6. Anticachectic effects of oral AR-42. (A) Upper panel, photographic images of representative leg skeletal muscles in the right hind limb; lower panel, H&E staining of represented frozen cross-sectional gastrocnemius muscle fibers of $KP^{fl/fl}C$ mice treated with AR-42 (25 mg/kg) or vehicle. (B) The cross-sectional area of muscle fiber diameter is represented as a stacked column. The number of fibers >1800μm^2 in gastrocnemius muscles in $KP^{fl/fl}C$ mice treated with AR-42 (25 mg/kg) was significantly greater than vehicle-treated mice (***$P < .001$, χ^2 test). (C) Treatment with AR-42 resulted in a significant improvement in grip strength from week 4 to week 8 (*$P < .05$), whereas vehicle-treated mice showed a significant decrease in grip strength from week 4 to week 8 (*$P < .05$). Grip strength was significantly increased in the AR-42–treated group versus vehicle at week 8 in $KP^{fl/fl}C$ mice (**$P < .01$). (D) Treatment with AR-42 resulted in decreased expression of the cachexia biomarker MuRF1 and increased expression of the HDAC inhibition marker acetylated histone H3.

determinants of this resistance may be useful in identifying responsive patient subpopulations.

These *in vitro* antiproliferative effects of AR-42 were reflected in our *in vivo* studies, in which oral AR-42 suppressed tumor growth in both the subcutaneous AsPC-1 xenograft tumor model and the genetically engineered $KP^{fl/fl}C$ model of pancreatic cancer. This tumor suppression was associated with changes in intratumoral biomarkers that reflected drug effects observed *in vitro*. These included proapoptotic changes in the expression of BCL-X_L and BAK and antiproliferative changes in c-Myc, PCNA, and cyclin B1 expression, which were associated with biomarkers of HDAC inhibition.

From a translational perspective, AR-42's antitumor activity in $KP^{fl/fl}C$ mice is noteworthy in that this model was engineered to harbor genetic lesions in the pancreas that have been shown to contribute to pancreatic carcinogenesis and progression in people. Specifically, these mice carry an oncogenic mutation in codon 12 of KRAS, rendering it constitutively active, and p53 nullizygosity, which generates rapidly progressing and lethal adenocarcinomas in 100% of mice by 8 weeks of age [40]. This model recapitulates many aspects of the progression of PDAC development seen in pancreatic cancer patients. Equally important is that the combination of AR-42 with gemcitabine improved the overall survival of $KP^{fl/fl}C$ mice over that of mice treated with either agent alone. This combinatorial effect of AR-42 and gemcitabine on survival is reminiscent of the findings of a recent study reporting improved efficacy for the combination of gemcitabine and *nab*-paclitaxel [41] and suggests that AR-42 may provide additional benefit in a regimen combining AR-42, gemcitabine, and *nab*-paclitaxel.

Cachexia is a devastating condition that affects the majority of PDAC patients, resulting in reduced physical and respiratory function, immunity, chemotherapy response, and overall survival [42]. In particular, pancreatic cancer patients with cachexia have been shown to have a significantly reduced survival, and nearly one third of pancreatic cancer deaths are related to cachexia rather than tumor burden [43]. Reminiscent of its effects in colon and lung tumor models of cancer cachexia [23], our data show that AR-42 can improve muscle function and mass, as determined by measurements of grip strength and muscle fiber size, respectively, suggesting that AR-42 also exhibits anticachectic activity in a model of pancreatic cancer. Future studies will more thoroughly characterize cachexia and the ability of AR-42 to diminish muscle wasting in pancreatic cancer.

Conclusion

In conclusion, this study demonstrates the efficacy of AR-42 in suppressing pancreatic tumor growth through modulation of apoptosis, HDAC inhibition, and cell growth and proliferation and, in combination with the standard of care gemcitabine, in prolonging overall survival in a spontaneous tumor model of pancreatic carcinogenesis. Together, these results suggest that the inclusion of AR-42 in therapeutic regimens represents a promising strategy for the treatment of pancreatic cancer.

Supplementary data to this article can be found online at http://dx.doi.org/10.1016/j.neo.2016.10.003.

Acknowledgements

The authors thank the Tissue Culture Shared Resource of Georgetown Lombardi Comprehensive Cancer Center (Washington, D.C.) for providing the COLO-357 pancreatic cancer cell line. The authors acknowledge the assistance of Pei-Rong Gu (National Cheng Kung University, Taiwan) and the following core facilities: OSU Comprehensive Cancer Center (CCC) Target Validation Shared Resource, OSU-CCC Analytical Cytometry core, National Cheng Kung University (NCKU)-Animal Center, and NCKU Hospital-Clinical Medicine Research Center (Proteomics/microscopy/tissue-bank). The authors also thank Dr. Po-Min Chiang (NCKU, Taiwan) for pathological consultations.

References

[1] Siegel RL, Miller KD, and Jemal A (2015). Cancer statistics, 2015. *CA Cancer J Clin* **65**(1), 5–29.

[2] Von Hoff DD, Ervin T, Arena FP, Chiorean EG, Infante J, Moore M, Seay T, Tjulandin SA, Ma WW, Saleh MN, et al (2013). Increased survival in pancreatic cancer with nab-paclitaxel plus gemcitabine. *N Engl J Med* **369**(18), 1691–1703.

[3] Koutsounas I, Giaginis C, Patsouris E, and Theocharis S (2013). Current evidence for histone deacetylase inhibitors in pancreatic cancer. *World J Gastroenterol* **19**(6), 813–828.

[4] Burris III HA, Moore MJ, Andersen J, Green MR, Rothenberg ML, Modiano MR, Cripps MC, Portenoy RK, Storniolo AM, Tarassoff P, et al (1997). Improvements in survival and clinical benefit with gemcitabine as first-line therapy for patients with advanced pancreas cancer: a randomized trial. *J Clin Oncol* **15**(6), 2403–2413.

[5] Mahaseth H, Brutcher E, Kauh J, Hawk N, Kim S, Chen Z, Kooby DA, Maithel SK, Landry J, and El-Rayes BF (2013). Modified FOLFIRINOX regimen with improved safety and maintained efficacy in pancreatic adenocarcinoma. *Pancreas* **42**(8), 1311–1315.

[6] Sharma S, Kelly TK, and Jones PA (2010). Epigenetics in cancer. *Carcinogenesis* **31**(1), 27–36.

[7] Falkenberg KJ and Johnstone RW (2014). Histone deacetylases and their inhibitors in cancer, neurological diseases and immune disorders. *Nat Rev Drug Discov* **13**(9), 673–691.

[8] Zhang T, Chen Y, Li J, Yang F, Wu H, Dai F, Hu M, Lu X, Peng Y, Liu M, et al (2014). Antitumor action of a novel histone deacetylase inhibitor, YF479, in breast cancer. *Neoplasia* **16**(8), 665–677.

[9] Donadelli M, Costanzo C, Faggioli L, Scupoli MT, Moore PS, Bass C, Scarpa A, and Palmieri M (2003). Trichostatin A, an inhibitor of histone deacetylases, strongly suppresses growth of pancreatic adenocarcinoma cells. *Mol Carcinog* **38**(2), 59–69.

[10] Kumagai T, Wakimoto N, Yin D, Gery S, Kawamata N, Takai N, Komatsu N, Chumakov A, Imai Y, and Koeffler HP (2007). Histone deacetylase inhibitor, suberoylanilide hydroxamic acid (Vorinostat, SAHA) profoundly inhibits the growth of human pancreatic cancer cells. *Int J Cancer* **121**(3), 656–665.

[11] Arnold NB, Arkus N, Gunn J, and Korc M (2007). The histone deacetylase inhibitor suberoylanilide hydroxamic acid induces growth inhibition and enhances gemcitabine-induced cell death in pancreatic cancer. *Clin Cancer Res* **13**(1), 18–26.

[12] Qiao Z, Ren S, Li W, Wang X, He M, Guo Y, Sun L, He Y, Ge Y, and Yu Q (2013). Chidamide, a novel histone deacetylase inhibitor, synergistically enhances gemcitabine cytotoxicity in pancreatic cancer cells. *Biochem Biophys Res Commun* **434**(1), 95–101.

[13] Lu Q, Wang DS, Chen CS, Hu YD, and Chen CS (2005). Structure-based optimization of phenylbutyrate-derived histone deacetylase inhibitors. *J Med Chem* **48**(17), 5530–5535.

[14] Kulp SK, Chen CS, Wang DS, Chen CY, and Chen CS (2006). Antitumor effects of a novel phenylbutyrate-based histone deacetylase inhibitor, (S)-HDAC-42, in prostate cancer. *Clin Cancer Res* **12**(17), 5199–5206.

[15] Lu YS, Kashida Y, Kulp SK, Wang YC, Wang D, Hung JH, Tang M, Lin ZZ, Chen TJ, Cheng AL, et al (2007). Efficacy of a novel histone deacetylase inhibitor in murine models of hepatocellular carcinoma. *Hepatology* **46**(4), 1119–1130.

[16] Yang YT, Balch C, Kulp SK, Mand MR, Nephew KP, and Chen CS (2009). A rationally designed histone deacetylase inhibitor with distinct antitumor activity against ovarian cancer. *Neoplasia* **11**(6), 552–563 [3 p following 63].

[17] Lin TY, Fenger J, Murahari S, Bear MD, Kulp SK, Wang D, Chen CS, Kisseberth WC, and London CA (2010). AR-42, a novel HDAC inhibitor, exhibits biologic activity against malignant mast cell lines via down-regulation of constitutively activated Kit. *Blood* **115**(21), 4217–4225.

[18] Sargeant AM, Rengel RC, Kulp SK, Klein RD, Clinton SK, Wang YC, and Chen CS (2008). OSU-HDAC42, a histone deacetylase inhibitor, blocks prostate

tumor progression in the transgenic adenocarcinoma of the mouse prostate model. *Cancer Res* **68**(10), 3999–4009.

[19] Chen CS, Weng SC, Tseng PH, Lin HP, and Chen CS (2005). Histone acetylation-independent effect of histone deacetylase inhibitors on Akt through the reshuffling of protein phosphatase 1 complexes. *J Biol Chem* **280**(46), 38879–38887.

[20] Zhang S, Suvannasankha A, Crean CD, White VL, Chen CS, and Farag SS (2011). The novel histone deacetylase inhibitor, AR-42, inhibits gp130/Stat3 pathway and induces apoptosis and cell cycle arrest in multiple myeloma cells. *Int J Cancer* **129**(1), 204–213.

[21] Chen CS, Wang YC, Yang HC, Huang PH, Kulp SK, Yang CC, Lu YS, Matsuyama S, Chen CY, and Chen CS (2007). Histone deacetylase inhibitors sensitize prostate cancer cells to agents that produce DNA double-strand breaks by targeting Ku70 acetylation. *Cancer Res* **67**(11), 5318–5327.

[22] Chen MC, Chen CH, Chuang HC, Kulp SK, Teng CM, and Chen CS (2011). Novel mechanism by which histone deacetylase inhibitors facilitate topoisomerase IIalpha degradation in hepatocellular carcinoma cells. *Hepatology* **53**(1), 148–159.

[23] Tseng YC, Kulp SK, Lai IL, Hsu EC, He WA, Frankhouser DE, Yan PS, Mo X, Bloomston M, Lesinski GB, et al (2015). Preclinical investigation of the novel histone deacetylase inhibitor AR-42 in the treatment of cancer-induced cachexia. *J Natl Cancer Inst* **107**(12).

[24] Fearon KC, Glass DJ, and Guttridge DC (2012). Cancer cachexia: mediators, signaling, and metabolic pathways. *Cell Metab* **16**(2), 153–166.

[25] Wigmore SJ, Plester CE, Richardson RA, and Fearon KC (1997). Changes in nutritional status associated with unresectable pancreatic cancer. *Br J Cancer* **75**(1), 106–109.

[26] Riccardi C and Nicoletti I (2006). Analysis of apoptosis by propidium iodide staining and flow cytometry. *Nat Protoc* **1**(3), 1458–1461.

[27] Schneider CA, Rasband WS, and Eliceiri KW (2012). NIH Image to Image J: 25 years of image analysis. *Nat Methods* **9**(7), 671–675.

[28] Cheng H, Xie Z, Jones WP, Wei XT, Liu Z, Wang D, Coss CC, Chen CS, Marcucci G, Garzon R, et al (2016). Preclinical pharmacokinetics study of R- and S-enantiomers of the histone deacetylase inhibitor, AR-42 (NSC 731438), in rodents. *AAPS J* **18**(3), 737–745.

[29] Huang PH, Lu PJ, Ding LY, Chu PC, Hsu WY, Chen CS, Tsao CC, Chen BH, Lee CT, and Shan YS, et al (2016). TGFβ promotes mesenchymal phenotype of pancreatic cancer cells, in part, through epigenetic activation of VAV1. *Oncogene* .

[30] Feng W, Zhang B, Cai D, and Zou X (2014). Therapeutic potential of histone deacetylase inhibitors in pancreatic cancer. *Cancer Lett* **347**(2), 183–190.

[31] Hamacher R, Schmid RM, Saur D, and Schneider G (2008). Apoptotic pathways in pancreatic ductal adenocarcinoma. *Mol Cancer* **7**, 64.

[32] Bai J, Sui J, Demirjian A, Vollmer Jr CM, Marasco W, and Callery MP (2005). Predominant Bcl-XL knockdown disables antiapoptotic mechanisms: tumor necrosis factor-related apoptosis-inducing ligand-based triple chemotherapy overcomes chemoresistance in pancreatic cancer cells in vitro. *Cancer Res* **65**(6), 2344–2352.

[33] Albury TM, Pandey V, Gitto SB, Dominguez L, Spinel LP, Talarchek J, Klein-Szanto AJ, Testa JR, and Altomare DA (2015). Constitutively active Akt1 cooperates with KRas(G12D) to accelerate in vivo pancreatic tumor onset and progression. *Neoplasia* **17**(2), 175–182.

[34] Wong MH, Xue A, Baxter RC, Pavlakis N, and Smith RC (2016). Upstream and downstream co-inhibition of mitogen-activated protein kinase and PI3K/Akt/m-TOR pathways in pancreatic ductal adenocarcinoma. *Neoplasia* **18**(7), 425–435.

[35] He C, Jiang H, Geng S, Sheng H, Shen X, Zhang X, Zhu S, Chen X, Yang C, and Gao H (2014). Expression and prognostic value of c-Myc and Fas (CD95/APO1) in patients with pancreatic cancer. *Int J Clin Exp Pathol* **7**(2), 742–750.

[36] Yuan J, Kramer A, Matthess Y, Yan R, Spankuch B, Gatje R, Knecht R, Kaufmann M, and Strebhardt K (2006). Stable gene silencing of cyclin B1 in tumor cells increases susceptibility to taxol and leads to growth arrest in vivo. *Oncogene* **25**(12), 1753–1762.

[37] Yu M, Zhan Q, and Finn OJ (2002). Immune recognition of cyclin B1 as a tumor antigen is a result of its overexpression in human tumors that is caused by non-functional p53. *Mol Immunol* **38**(12–13), 981–987.

[38] Morton JP, Timpson P, Karim SA, Ridgway RA, Athineos D, Doyle B, Jamieson NB, Olen KA, Lowy AM, Brunton VG, et al (2010). Mutant p53 drives metastasis and overcomes growth arrest/senescence in pancreatic cancer. *Proc Natl Acad Sci U S A* **107**(1), 246–251.

[39] Mehdi O, Francoise S, Sofia CL, Urs G, Kevin Z, Bernard S, Igor S, Anabela CD, Dominique L, Eric M, et al (2012). HDAC gene expression in pancreatic tumor cell lines following treatment with the HDAC inhibitors panobinostat (LBH589) and trichostatine (TSA). *Pancreatology* **12**(2), 146–155.

[40] Bardeesy N, Aguirre AJ, Chu GC, Cheng KH, Lopez LV, Hezel AF, Feng B, Brennan C, Weissleder R, Mahmood U, et al (2006). Both p16(Ink4a) and the p19(Arf)-p53 pathway constrain progression of pancreatic adenocarcinoma in the mouse. *Proc Natl Acad Sci U S A* **103**(15), 5947–5952.

[41] Frese KK, Neesse A, Cook N, Bapiro TE, Lolkema MP, Jodrell DI, and Tuveson DA (2012). nab-Paclitaxel potentiates gemcitabine activity by reducing cytidine deaminase levels in a mouse model of pancreatic cancer. *Cancer Discov* **2**(3), 260–269.

[42] Prado CM, Bekaii-Saab T, Doyle LA, Shrestha S, Ghosh S, Baracos VE, and Sawyer MB (2012). Skeletal muscle anabolism is a side effect of therapy with the MEK inhibitor: selumetinib in patients with cholangiocarcinoma. *Br J Cancer* **106**(10), 1583–1586.

[43] Bachmann J, Ketterer K, Marsch C, Fechtner K, Krakowski-Roosen H, Buchler MW, Friess H, and Martignoni ME (2009). Pancreatic cancer related cachexia: influence on metabolism and correlation to weight loss and pulmonary function. *BMC Cancer* **9**, 255.